Multiphonon resonant Raman scattering in MoS_2

K. Gołasa,[1,a)] M. Grzeszczyk,[1] P. Leszczyński,[2] C. Faugeras,[2] A. A. L. Nicolet,[2] A. Wysmołek,[1] M. Potemski,[2] and A. Babiński[1]
[1]*Faculty of Physics, University of Warsaw, ul. Hoża 69, 00-681 Warszawa, Poland*
[2]*Laboratoire National des Champs Magnétiques Intenses, CNRS-UJF-UPS-INSA, 25, avenue des Martyrs, 38042 Grenoble, France*

(Received 21 December 2013; accepted 20 February 2014; published online 5 March 2014)

Optical emission spectrum of a resonantly ($\lambda = 632.8$ nm) excited molybdenum disulfide (MoS_2) is studied at liquid helium temperature. More than 20 peaks in the energy range spanning up to 1400 cm^{-1} from the laser line, which are related to multiphonon resonant Raman scattering processes, are observed. The attribution of the observed lines involving basic lattice vibrational modes of MoS_2 and both the longitudinal ($LA(M)$) and the transverse ($TA(M)$ and/or $ZA(M)$) acoustic phonons from the vicinity of the high-symmetry M point of the MoS_2 Brillouin zone is proposed. © *2014 AIP Publishing LLC*. [http://dx.doi.org/10.1063/1.4867502]

One of the intensely investigated areas of the material research in recent years is the study of low dimensional structures with a seminal example of graphene.[1] Along the line, a lot of interest is devoted to transition metal dichalcogenides—compounds in which layers of strongly covalently bound X-M-X atoms are relatively weakly bound by van der Waals forces. Properties of the compounds have been studied using numerous techniques for last 50 years.[2] Molybdenum disulfide (MoS_2) is a member of the family. Bulk MoS_2 is a semiconductor with an indirect gap equal to 1.29 eV at room temperature. The lowest energy direct optical transition in bulk MoS_2 takes place at the high-symmetry point K of the Brillouin zone (BZ) at 1.8 eV (at room temperature). Bulk MoS_2 has been used for years in industrial machinery for lubrication.[4] A strong optical absorption of MoS_2 in the solar spectral range and a high stability against photocorrosion makes it also of great interest for photovoltaic[5] and photocatalytic applications.[6] The layered structure of MoS_2 makes it relatively easy to obtain monolayer samples, which properties substantially differ from the properties of bulk material.[3] The indirect band-gap of MoS_2 was found to increase significantly with the decreasing number of layers resulting in the direct band-gap in a monolayer sample. Several applications of monolayer MoS_2 have recently been proposed in the field effect transistors,[7] the logical circuits,[8] and the optoelectronic devices.[9] The interest in the applications and fascinating physics of these really two-dimensional systems make the comprehensive understanding of the MoS_2 properties very important. One of the areas of interest is the MoS_2 lattice dynamics. Raman scattering spectroscopy is a technique of choice to study the properties. The non-resonant Raman spectrum is dominated by two basic vibrational modes: E^1_{2g} which results from in-plane vibrations of two S atoms with respect to the Mo atom and A_{1g} which is due to the out-of-plane vibrations of S atoms in opposite directions. The sensitivity of those peaks to the number of layers has recently been employed in a standard method of a thin MoS_2 layer characterization.[10] More complex is the optical spectrum due to the resonant excitation of MoS_2. In that case second-order Raman scattering processes, which are enhanced by the coupling of phonon modes to electronic states excited optically in the crystal, are more effective than the modes related to the first-order Raman scattering. There are several reports on the resonant Raman scattering in bulk[11–18] and a few monolayer MoS_2 samples.[19,20] There is a general agreement on the attribution of the peaks observed in the resonantly excited Raman scattering spectrum to vibrational modes and their replica involving the longitudinal acoustic phonon $LA(M)$.[21] The attribution of the involved phonon to M point of the BZ is based on neutron scattering measurements.[22]

In order to get a deeper insight into the lattice dynamics of MoS_2, we performed measurements of the resonantly excited optical emission spectrum at low temperature in a broad (up to 1400 cm^{-1} from the laser line) energy range. Although main features of the spectrum are visible already at $T = 77$ K, our measurements were done at liquid helium temperature ($T = 4.2$ K) in order to provide better stability of our experimental setup. We analyze the spectrum and we propose an alternative attribution of the observed peaks which involves both longitudinal and *transverse* acoustic phonons. Using the attribution, we explain most details of the spectrum. Our results point out to substantial enhancement of electron-phonon interaction at M point of the BZ.

Microscopic measurements of optical spectra were performed in a backscattering geometry with a resonant and a non-resonant excitation. For the resonance Raman spectra, the 632.8 nm (1.96 eV) line of a He-Ne laser was used and for higher energy excitation a continuous-wave 532 nm (2.33 eV) solid-state laser was employed. All measurements were carried out with an optical filter used to avoid local heating effect by reducing the incident power to roughly 0.8 mW. The laser light spot on the sample was equal to ~1 μm. An Olympus MPlan N microscope 100 ×/0.90 objective was used to both excite the sample and collect the emitted light. The collected spectra were dispersed by a Horiba-Yobin T64000 Series II micro-Raman system, equipped with a multichannel high-resolution Si-charge coupled device. For the low-temperature measurements, a continuous flow Oxford Instruments cryostat accommodated with an optical window

a)Electronic mail: Katarzyna.Golasa@fuw.edu.pl

was used. The investigated sample was kept in vacuum (pressure lower that 10^{-5} bar) on a cold finger of the cryostat in a close proximity (a few mm) to the optical window. The investigated sample was prepared using mechanical exfoliation[23] from molybdenite, a specimen of natural molybdenum ore from Molly Hill deposit in Canada on a Si/75 nm SiO_2 substrate.

The Raman spectra of bulk MoS_2 measured at room temperature are shown in Fig. 1. The most intense peaks in the non-resonantly excited spectrum (see Fig. 1(a)) are related to two previously mentioned vibrational modes: E^1_{2g} (384 cm^{-1}) and A_{1g} (409 cm^{-1}). Two other Raman-active modes of the MoS_2 lattice vibrations are E_{1g} at 286 cm^{-1} which is forbidden in the backscattering geometry and hardly observed in our spectrum and E^2_{2g} mode at 32 cm^{-1} which is outside our experimentally accessible energy range.[17] The A_{1g} and E^1_{2g} peaks are less intensive in the spectrum excited close to the resonance with direct band-gap of bulk MoS_2 (see Fig. 1(b)). The peaks related to the second-order Raman scattering become more intense with such an excitation than the modes resulting from first-order processes. The most pronounced peak of the resonance Raman spectrum is a double-mode feature at 465 cm^{-1}. Both modes comprising the peak are only weakly observable in the non-resonant Raman spectrum. The double structure of that peak was first suggested by Frey *et al.*[17] and attributed to a combined process involving two longitudinal acoustic phonons from the edge of the BZ (2 $LA(M)$) and the normally IR-active $A_{2u}(\Gamma)$ phonon mode. Two more features present in the resonant Raman spectrum are usually attributed to the higher order processes: $2E_{1g}(\Gamma)$ at$\sim$572 cm^{-1} and $E^1_{2g}(M)+LA(M)$ at $\sim$600 cm^{-1}. Peaks observed at $\sim$178 cm^{-1} and $\sim$643 cm^{-1} are usually[16] attributed to combined processes: $A_{1g}(M)-LA(M)$ and $A_{1g}(M)+LA(M)$. Their energies can be used to estimate the energies of the respective modes: $LA(M)$ − 232.5 cm^{-1} and $A_{1g}(M)$ − 410.5 cm^{-1}. The energy of the $LA(M)$ phonon determined from the procedure is somewhat larger than the value determined from the energy of 2 $LA(M)$ peak in the non-resonant spectrum (226.3 cm^{-1}). The origin of the difference will be addressed later in this work. The energy of the $A_{1g}(M)$ mode corresponds to the energy of the $A_{1g}(\Gamma)$ (409 cm^{-1}) which reflects the dispersionless character of this mode dependence on the crystal momentum along the $\Gamma-M$ direction[22,24] of the BZ. Similarly, estimated energy of the $E^1_{2g}(M)$ mode (367.5 cm^{-1}) is smaller than the energy of the $E^1_{2g}(\Gamma)$ mode (384 cm^{-1}), which is coherent with the theoretical calculations.[24] Finally, the mode "b" observed at $\sim$420 cm^{-1} is attributed to a two-phonon Raman process involving the successive emission of a dispersive quasi-acoustic (QA) phonon and a dispersionless TO phonon along the c-axis (Ref. 16). It is interesting to note that no spectral feature at $\sim$230 cm^{-1} related to the disorder-allowed first-order process[25] can be observed in the spectrum. The feature corresponds to the scattering process with a single $LA(M)$ phonon as it was previously observed, e.g., in MoS_2 nanoparticles[17] and thin MoS_2 layers.[26] Lack of this feature may confirm relatively good quality of our natural sample.

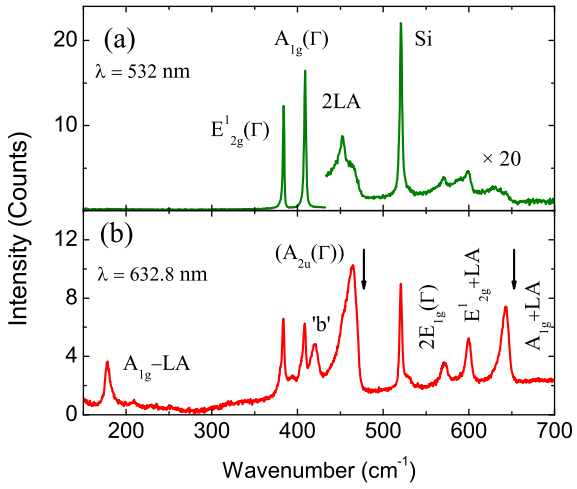

FIG. 1. Optical spectra of bulk MoS_2 excited at room temperature non-resonantly - note the enlarged intensity of the high-energy part of the spectrum (a) and resonantly (b). The high energy edges of peaks at $\sim$465 cm^{-1} and $\sim$643 cm^{-1} are denoted with arrows. The attributed phonons originate from M point of the Brillouin zone unless stated otherwise.

Important for our further analysis is the observation that the characteristic high energy cut-off shape of the 465 cm^{-1} peak closely resembles the shape of a higher-order scattering peak at $\sim$643 cm^{-1} (see Fig. 1(b)). This similarity is seen with both excitation regimes. Because of a good numerical agreement it would be tempting to assign the latter peak to a combined process involving the 465 cm^{-1} phonon and a phonon of the energy $\sim$180 cm^{-1}. For the sake of the current study, the phonon will be referred to as XA. The XA mode cannot be related to a peak visible at room temperature at $\sim$178 cm^{-1} which is attributed to the differential process $A_{1g}(M)-LA(M)$.[15] The intensity of a differential process with a creation of a phonon of the energy $\hbar\omega_1$ and annihilation of a phonon of the energy $\hbar\omega_2$ is proportional to $n(1,T)*(n(2,T)+1)$, where $n(i,T)=(\exp(\hbar\omega_i/kT)-1))^{-1}$.[15] Thus, the Raman peak related to the differential process is expected to disappear at low temperature ($\hbar\omega_1 > kT$) which is indeed seen in Fig. 2(b). The observed temperature dependence of the peak at 178 cm^{-1} supports its assignment to the differential process $A_{1g}(M)-LA(M)$ and excludes its assignment to the XA mode.

We propose another attribution of the XA phonon. In our opinion, the phonon in question is related to the transverse acoustic (TA) and/or out-of-plane acoustic (ZA) mode.[24] The dispersion of both modes flattens at the border of the BZ near the high-symmetry M point, leading to the substantial increase in the phonon density of states at $\sim$180 cm^{-1}.

To prove the hypothesis, we analyzed in details the optical spectrum excited resonantly ($\lambda=632.8$ nm) at low ($T=4.2$ K) temperature (see Fig. 2). The temperature-induced shift of the background photoluminescence from 1.8 eV at $T=300$ K to 1.9 eV at $T=4.2$ K can be noticed in the spectra. There are more well-resolved peaks observed in the low temperature spectrum in a broad energy range spanning up to 1400 cm^{-1} from the laser line energy (see Fig. 2(b)) as compared to the room temperature spectrum (see Fig. 2(a)). Substantial changes at the low energy (below 400 cm^{-1}) can also be seen. In this work, we will focus on the high-energy range of the spectrum.

At the high-energy end of the spectrum a series of three similar features can be observed at energies 929.5 cm^{-1},

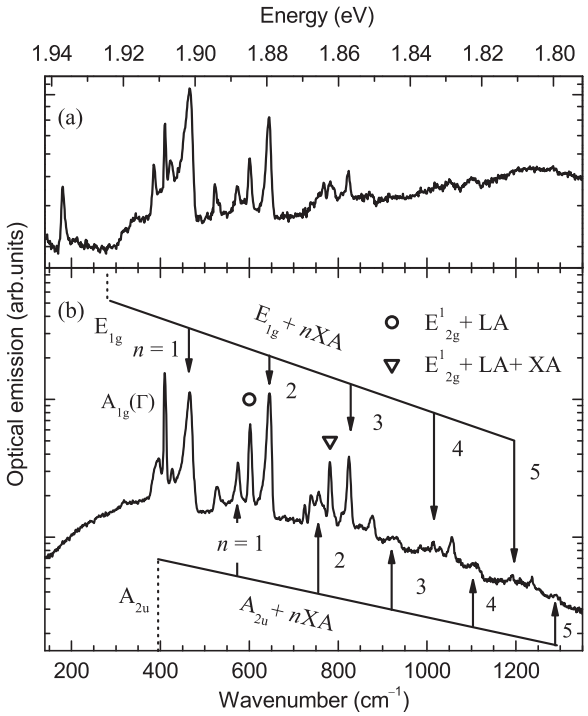

FIG. 2. Optical spectrum of MoS_2 resonantly excited at room temperature (a) and at low temperature ($T = 4.2$ K) (b). The attributed phonons originate from M point of the Brillouin zone unless stated otherwise.

1107.5 cm^{-1}, and 1289.5 cm^{-1}. We attribute the features to the three-, four-, and five-$XA(M)$ phonon replica of the $A_{2u}(M)$ phonon. We believe that also the peak at ~574 cm^{-1} belongs to the series. The linear fit to these four energies allows us to determine the energy of the $XA(M)$ phonon at 178.6 cm^{-1} and the energy of the $A_{2u}(M)$ mode at 394.2 cm^{-1}. Using the values it is possible to predict the $A_{2u}(M) + 2XA(M)$ replica at ~750.5 cm^{-1}, where in fact a broad feature can be seen as a background to three sharp peaks. Our attribution corresponds to the dispersive character of the A_{2u} phonon, which is due to asymmetric translation of both Mo and S atoms in the c-axis direction. The energy of the $A_{2u}(M)$ mode is substantially lower[24] than the energy of the $A_{2u}(\Gamma)$ mode (~470 cm^{-1} at room temperature), determined from reflectivity measurements.[12]

The energy of the $XA(M)$ phonon well explains the previously mentioned similarity of peaks observed at low temperature at ~466 cm^{-1} and ~645 cm^{-1} (see Figs. 3(a) and 3(b)). The lineshape analysis of these peaks as well as of the peak at ~825 cm^{-1} (see Fig. 3(c)) suggests that each peak is composed of two peaks of similar energies. We propose the attribution of the stronger components of those peaks to $XA(M)$ phonon replicas of the $E_{1g}(M)$ mode, namely: $E_{1g}(M) + XA(M)$ at ~466 cm^{-1}, $E_{1g}(M) + 2XA(M)$ at ~646.5 cm^{-1}, and $E_{1g}(M) + 3XA(M)$ at ~825 cm^{-1} and their weaker counterparts to 2 $LA(M)$ at 460 cm^{-1}, $A_{1g}(M) + LA(M)$ at ~643 cm^{-1}, and $A_{1g}(M) + LA(M) + XA(M)$ at ~822 cm^{-1}. This attribution allows us to determine the energy of the $E_{1g}(M)$ mode as 289 cm^{-1}. It may be noted that according to theoretical results presented in Ref. 24 the mode E_{1g} increases its energy along the $\Gamma - M$ direction and the theoretically predicted energy of the $E_{1g}(M)$ mode is higher than 300 cm^{-1}. However in the theoretical dispersion presented by Wakabayashi *et al.*,[22] the Σ_2 mode (corresponding to the E_{1g}) is practically dispersionless and the energy of the $E_{1g}(M)$ mode estimated from the dispersion equals 294 cm^{-1} which is in reasonable agreement with our estimate.

The bimodal lineshape of the peak at ~645 cm^{-1} (compare Fig. 3(b)) also explains the previously mentioned discrepancy between the $LA(M)$ phonon energy determined at room temperature from the resonant spectrum (232.5 cm^{-1}) and the non-resonant spectrum (226.3 cm^{-1}). The lineshape analysis of the peak observed at room temperature at 643 cm^{-1} allows us to determine the energy of the $A_{1g}(M) + LA(M)$ mode as 639 cm^{-1} and the resulted energy of the $LA(M)$ phonon as 230.5 cm^{-1}, which approaches the value determined from the non-resonant spectrum.

Introducing the $XA(M)$ phonon into the picture would also allow us to relate the peak at ~782 cm^{-1} which appears to be a replica of the previously identified $E^1_{2g}(M) + LA(M)$ mode at ~602.5 cm^{-1} (Ref. 17) (compare Fig. 3(c)) as a peak due to a combined process: $E^1_{2g}(M) + LA(M) + XA(M)$.

The main advantage of our model is its simplicity. Using our attribution several peaks in the resonantly excited optical spectrum of bulk MoS_2 can be ascribed to multiphonon processes involving phonons from the vicinity of M point of the BZ. It is to be noted that according to our attribution no spectral features corresponding to single phonons from M point of the BZ can be seen in the spectrum which is in line with the crystal momentum conservation principle

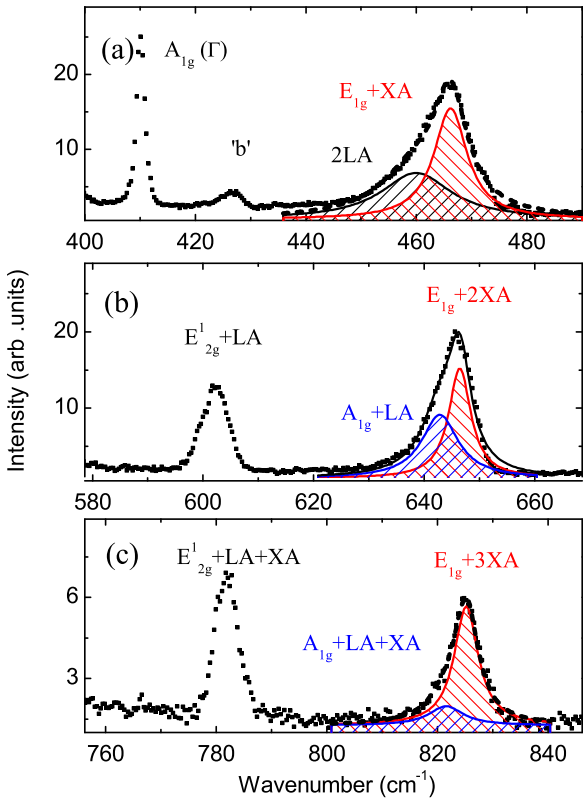

FIG. 3. Details of the optical spectra of bulk MoS_2 measured at low temperature. The broadened peaks were deconvoluted to show Lorentzian waveform contributions. The energy scales of consecutive panels are shifted by 178.6 cm^{-1} for more clarity. The attributed phonons originate from M point of the Brillouin zone unless stated otherwise.

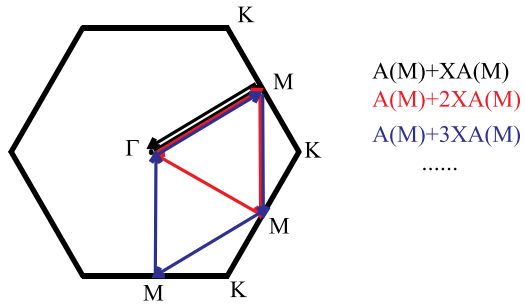

FIG. 4. Schematic diagram of the momentum conservation in the multiply emission of phonons from the *M* point of the MoS_2 Brillouin zone. *A* stands for a vibrational mode (E_{1g}, A_{2u}, A_{1g}, E^1_{2g}) or a phonon (*LA*, *XA*).

(see Fig. 4). Simultaneously, the multiple emission of consecutive two or more phonons from the *M*-point of the BZ obeys the momentum conservation rule (with a small uncertainty related to momentum of electron-hole pair to be lost in the resonant process). The presence of the multiphonon replica in the spectrum also supports our attribution of the involved *XA* phonon to *M* point of the BZ. Although both (*ZA* and *TA*) transverse modes are almost dispersionless between *M* and *K* points of the BZ, the need to conserve the momentum points out to *M* point as the origin of the XA phonon. We are aware that our model should be supported by a more strict theoretical analysis, which is beyond the scope of this experimental study and we believe that our experimental results will trigger the theoretical studies of the problem.

Our results can also be analyzed in terms of the mechanism responsible for the observed optical emission. In fact such a multiphonon resonant Raman scattering, with a cascade emission of phonons can be regarded as a form of a hot luminescence process.[27] However, the distinction between the two processes is impossible without measuring the emitted photons coherence.[28]

In conclusion, we studied the resonantly excited optical spectrum of bulk MoS_2 at low temperature. The spectrum was found to comprise several peaks, which were attributed to the multiphonon resonant Raman scattering process involving the *LA*(*M*) and the *TA*(*M*) and/or *ZA*(*M*) phonon replicas of vibrational modes from M points of the Brillouin zone. The energies of the phonons were determined and found to agree with theoretical predictions.

This work has been supported in part by Polish Funds for Science. Funding from European Graphene Flagship and European Research Council (ERC-2012-AdG-320590-MOMB) is also acknowledged.

[1]A. K. Geim and K. Novoselov, Nature Mater. **6**, 183 (2007).
[2]J. A. Wilson and A. D. Yoffe, Adv. Phys. **18**, 193 (1969).
[3]S. Z. Butler, S. M. Hollen, L. Cao, Y. Cui, J. A. Gupta, H. R. Gutirrez, T. F. Heinz, S. S. Hong, J. Huang, A. F. Ismach *et al.*, ACS Nano **7**, 2898 (2013).
[4]M. R. Hilton and P. D. Fleischauer, in *American Society of Metals Handbook, Friction, Lubrication, and Wear Technology*, edited by S. D. Henry (ASM International, Materials Park, OH, 1992), Vol. 18, pp. 150.
[5]E. Gourmelon, O. Lignier, H. Hadouda, G. Couturier, J. C. Bernede, J. Teddb, J. Pouzet, and J. Salardenne, J. Sol. Energy Mater. Sol. Cells **46**, 115 (1997).
[6]W. K. Ho, J. C. Yu, J. Lin, J. Yu, and P. Li, Langmuir **20**, 5865 (2004).
[7]B. Radisavljevic, A. Radenovic, J. Brivio, V. Giacometti, and A. Kis, Nat. Nanotechnol. **6**, 147 (2011).
[8]B. Radisavljevic, M. B. Whitwick, and A. Kis, ACS Nano **5**, 9934 (2011).
[9]A. Splendiani, L. Sun, Y. Zhang, T. Li, J. Kim, C.-Y. Chim, G. Galli, and F. Wang, Nano Lett. **10**, 1271 (2010).
[10]C. Lee, H. Yan, L. E. Brus, T. F. Heinz, J. Hone, and S. Ryu, ACS Nano **4**, 2695 (2010).
[11]J. L. Verble and T. J. Wietling, Phys. Rev. Lett. **25**, 362 (1970).
[12]T. J. Wietling and J. L. Verble, Phys. Rev. B **3**, 4286 (1971).
[13]J. L. Verble, T. J. Wietling, and P. R. Reed, Solid State Commun. **11**, 941 (1972).
[14]O. P. Agnihotri, H. K. Sehgal, and A. K. Garg, Solid State Commun. **12**, 135 (1973).
[15]J. M. Chen and C. S. Wang, Solid State Commun. **14**, 857 (1974).
[16]T. Sekine, K. Uchinokura, T. Nakashizu, E. Matsuura, and R. Yoshizaki, J. Phys. Soc. Jpn. **53**, 811 (1984).
[17]G. L. Frey, R. Tenne, M. J. Matthiews, M. S. Dresselhaus, and G. Dresselhaus, Phys. Rev. B **60**, 2883 (1999).
[18]B. C. Windom, W. G. Sawyer, and D. W. Hahn, Tribol. Lett. **42**, 301 (2011).
[19]B. Chakraborty, H. S. S. Ramakrishna Matte, A. K. Sood, and C. N. R. Rao, J. Raman Spectr. **44**, 92 (2013).
[20]H. Li, Q. Zhang, Ch. Ch. R. Yap, B. K. Tay, T. H. T. Edwin, A. Olivier, and D. Baillargeat, Adv. Funct. Mater. **22**, 1385 (2012).
[21]A. M. Stacy and D. T. Hodul, J. Phys. Chem. Solids **46**, 405 (1985).
[22]N. Wakabayashi, H. G. Smith, and R. M. Nicklow, Phys. Rev. B **12**, 659 (1975).
[23]R. F. Frindt, Phys. Rev. **140**, A536 (1965).
[24]A. Molina-Sanchez and L. Wirtz, Phys. Rev. B **84**, 155413 (2011).
[25]N. T. McDevitt, J. S. Zabinski, M. S. Donley, and J. E. Bultman, Appl. Spectrosc. **48**, 733 (1994).
[26]K. Golasa, M. Grzeszczyk, K. P. Korona, R. Bozek, J. Binder, J. Szczytko, A. Wysmolek, and A. Babinski, Acta Phys. Pol., A **124**, 849 (2013).
[27]M. V. Klein, Phys. Rev. B **8**, 919 (1973).
[28]P. P. Yu and M. Cardona, *Fundamentals of Semiconductors: Physics and Materials Properties* (Springer-Verlag, Berlin, 1999).